Coupling Analysis of PCB-Chassis Systems with Signal Lines and Via Structures using SPICE

Naoki Kobayashi, Ken Morishita, Manabu Kusumoto
and Takashi Harada

System Jisso Research Laboratories
NEC Corporation
Sagamihara City, Japan

Todd Hubing

Holcombe Department of Electrical & Computer
Engineering
Clemson University
Clemson, SC 29634-0915, USA

Abstract— **This paper describes the SPICE modeling of printed circuit boards (PCBs) with signal lines and via structures electrically connected to a metal chassis. First, a PCB model is proposed considering the coupling between signal lines and the power bus due to via structures. Next, the model is expanded to include the chassis and grounding posts. The calculated results using SPICE are shown to be consistent with experimental data. Furthermore, positioning of the grounding posts near the edges of the PCB is shown experimentally and numerically to reduce radiated emissions.**

Keywords- **SPICE model; Radial/Coaxial line junction model; power bus resonance; chassis connections; grounding posts; equivalent magnetic current source; radiated EMI from PCBs**

I. INTRODUCTION

PCB-chassis systems include several structures that may couple electromagnetic energy away from the PCB resulting in radiated emissions. In particular, conductors penetrating various electromagnetic domains (e.g. via structures in a PCB or grounding posts connecting a PCB to a metal chassis) can facilitate unwanted coupling that results in the deterioration of signal waveforms, power bus resonances [1][2] and chassis cavity resonances [3]. Therefore, it is desirable to be able to model the coupling due to these structures in electronic designs.

In previously published work, analytical SPICE models of via structures through an arbitrary number of multiple planes were derived based on a radial/coaxial line junction model [4] [5]. Furthermore, SPICE was used to model boards with multiple layers in a PCB-chassis system where the power planes were parallel to the chassis and ground planes were connected to the chassis using grounding posts [3]. Although the calculated results from these models were shown to be consistent with the corresponding experimental data, these models did not include signal lines and via structures, which potentially could have a significant effect on the coupling processes.

This paper models PCB-chassis systems with signal lines and via structures using SPICE. Furthermore, the paper applies the proposed models to the investigation of the radiated emissions from these structures and investigates how the radiated EMI depends on the number and location of the grounding posts.

II. DESCRIPTION OF THE METHOD

This section describes a SPICE modeling procedure for a PCB-chassis system with signal lines and via structures. First, the SPICE model of the PCB consisting of a power bus, signal lines and via structures is developed by combining a power bus model with signal line models through via models, which are analytically obtained in SPICE format. Next, the SPICE model of the PCB-chassis system with signal lines and via structures is obtained by combining the PCB model with the chassis model through the grounding post models.

A. The SPICE model consisting of a power bus, signal lines and via structures

Figure 1(a) shows a simple printed circuit board consisting of a power bus and signal lines. The signal line consists of three microstrip configurations and two via structures. The via structures are the main source of coupling between the power bus and the signal line in this configuration. The block diagram for the SPICE modeling is represented as in Figure 1(b). The SPICE model for the power bus cavity is a 2-dimensional ladder network consisting of small planar segments [6]. The models for the microstrip lines are simple transmission line models where the circuit parameters are calculated analytically, or by using a 2-dimensional static field solver [7]. For the via structures, the SPICE models are analytically obtained based on the radial/coaxial line junction model in the following way.

Figure 2(a) shows a configuration where the coupling is superimposed on the radial/coaxial line junction model [5]. The input and output of the signal line correspond to the top and bottom sides of the coaxial line, respectively. The via structure in the power bus is modeled as a radial transmission line. Figure 2(b) shows the equivalent circuit of Figure 2(a) using susceptances, B_v, B_c, B_D and an ideal transformer with a turns ratio, R [5]. These parameters can be determined analytically

using mathematical functions with the parameters of inner and outer radii, a, b, permittivity, ε, permeability, μ, the thickness of the dielectric layer, h, and the frequency, f, as follows:

$$B_V = -\frac{2\pi}{\eta\ln\left(\dfrac{b}{a}\right)}\frac{1}{\sin(kh)} + 2\sum_{m=1}^{\infty}(-1)^m D_m$$

$$B_C = -\frac{2\pi}{\eta\ln\left(\dfrac{b}{a}\right)}\cot(kh) + 2\sum_{m=1}^{\infty}D_m - B_V,$$

$$B_D = \frac{2\pi a}{\eta h}\frac{J_1(ka)Y_0(kb)-J_0(kb)Y_1(ka)}{J_0(ka)Y_0(kb)-J_0(kb)Y_0(ka)},$$

$$R = \sqrt{\frac{2}{\pi}\ln\left(\frac{b}{a}\right)}\left\{\gamma_0\left[J_0(ka)Y_0(kb)-J_0(kb)Y_0(ka)\right]\right\}^{-\frac{1}{2}}$$

with

$$\gamma_0 = \frac{\pi}{2}\frac{1}{\ln(b/a)}\left[J_0(ka)Y_0(kb)-J_0(kb)Y_0(ka)\right]$$

$$D_m = \frac{2\pi}{\eta kh\ln^2(b/a)}\frac{1}{q_m^2}\frac{K_0(q_m kb)}{K_0(q_m ka)},$$

$$\times\left[I_0(q_m ka)K_0(q_m kb)-I_0(q_m kb)K_0(q_m ka)\right]$$

$$q_m = \sqrt{\left(\frac{m\pi}{kh}\right)^2 - 1},\, k = 2\pi f\sqrt{\varepsilon\mu},\, \eta = \sqrt{\frac{\mu}{\varepsilon}},$$

J_0, J_1 : Bessel Function of First Kind

Y_0, Y_1 : Bessel Function of Second Kind

K_0, I_0 : Modified Bessel Functions

Notice that the inner and outer radii, a and b, are the radii of the via-pin and clearance hole in the model, respectively.

Figure 2(c) shows the SPICE model of Figure 2(b) [4]. When the wavelength is much smaller than the thickness of the dielectric layer, h, these SPICE parameters can be approximately represented as shown in the following equations.

$$L_V = -\frac{1}{2\pi f B_V} \cong \frac{\mu h\ln\left(\dfrac{b}{a}\right)}{2\pi},\quad C_C = \frac{B_C}{2\pi f} \cong \frac{\pi\varepsilon h}{\ln\left(\dfrac{b}{a}\right)}$$

$$|L_D| = \left|\frac{1}{2\pi f B_D}\right| \cong \frac{\mu h\ln\left(\dfrac{b}{a}\right)}{2\pi},\quad R \cong 1$$

Notice that B_D can be represented using the inductance of $|L_D|$ and a current-controlled current source as indicated in Figure 2(c).

The overall SPICE model for the PCB configuration in Figure 1 is obtained using the via models at the connection points between the models for the power bus and transmission lines.
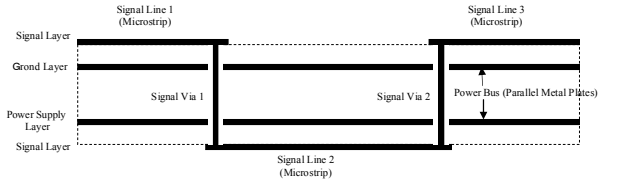
(a) The Configuration of the PCB including a power bus, signal lines and vias
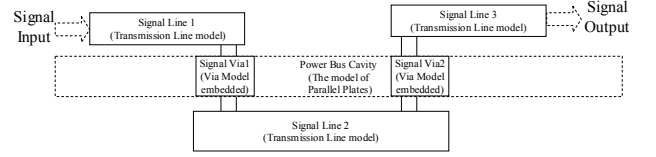
(b) Block Diagram of the SPICE model for the PCB including a power bus, signal lines and vias

Figure 1. Configuration of the PCB and its Block Diagram for the SPICE model.

B. The SPICE model of the PCB-chassis system with signal lines and via structures

Figure 3(a) shows a diagram of the PCB-chassis system where the PCB is mounted near and parallel to a metal chassis. When the PCB ground is electrically connected to the chassis by means of grounding posts through the power plane, the coupling from the power bus to the chassis affects the radiated EMI because a cavity antenna is formed between the bottom side of the PCB and the chassis [3]. A block diagram for the SPICE modeling is provided in Figure 3(b). The SPICE model for the chassis cavity is a 2-dimensional ladder network similar to the power bus cavity model. The SPICE models for the coupling between the power bus and chassis cavity through grounding posts is also analytically obtained by regarding the configuration as the series connection of two signal via models based on the radial/coaxial line junction model with the top and bottom coaxial line ports shorted. Figures 2(d) and (e) show the configuration and the equivalent circuit model, respectively. The susceptances, B_{V1}, B_{C1}, and B_{D1}, correspond to part of the power bus, and B_{V2}, B_{C2}, and B_{D2}, represent part of the chassis cavity.

Notice that the coupling between the microstrip line on the bottom side of the PCB and the chassis cavity is neglected in the model since the coupling is likely to be small compared to the direct coupling through the grounding posts.

If the cavity resonances are dominant sources of radiated emissions, the radiated EMI from the PCB-chassis system can be approximated by applying equivalent magnetic current sources along the power bus and chassis cavity walls [3]. In this case, the effect that the number and locations of grounding posts has on the radiated emissions can be investigated using the calculated results from the PCB-chassis system SPICE model. The mathematical formulation for the radiated electric field, $\mathbf{E}$, can

be obtained using the calculated voltages, V_1 and V_2 along the power bus and chassis cavity as follows [8];

$$\mathbf{E} = -\frac{1}{\varepsilon_0} \nabla \times \mathbf{F},$$

with

$$\mathbf{F} = \varepsilon_0 \frac{e^{-jk_0 r}}{4\pi r} \mathbf{L}$$

$$\mathbf{L} = \int_{S_1} \frac{V_1}{h_1} e^{jk_0 r' \cos\psi} d\mathbf{S}_1$$
$$+ \int_{S_2} \frac{V_2}{h_2} e^{jk_0 r' \cos\psi} d\mathbf{S}_2$$

$$k_0 = 2\pi f \sqrt{\varepsilon_0 \mu_0},$$

where ε_0 and μ_0 are the free-space permittivity and permeability. $\mathbf{S}_1$ and $\mathbf{S}_2$ represent the area element vector along the power bus wall with the height, h_1, and the chassis cavity walls with the height, h_2, respectively. r represents the distance from the origin of the coordinate system to the observation point at the far field. r' represents the distance from the origin to an infinitesimal area element inside the integral. ψ is the angle between the 2 line segments, the former of which is from the origin to the observation point and the latter is from the origin to the infinitesimal area element inside the integral.
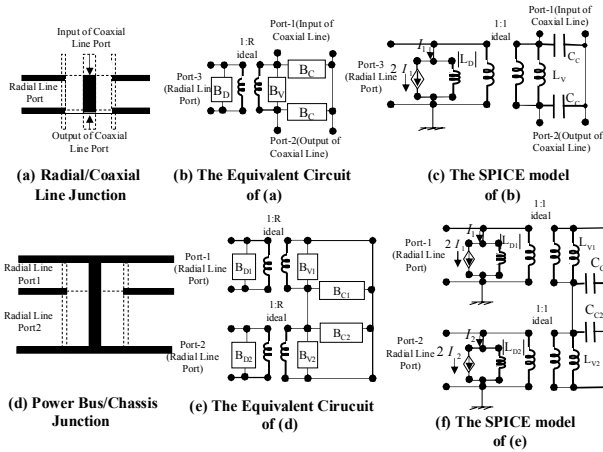
Figure 2. The SPICE modeling procedures for the via structures and grounding posts.
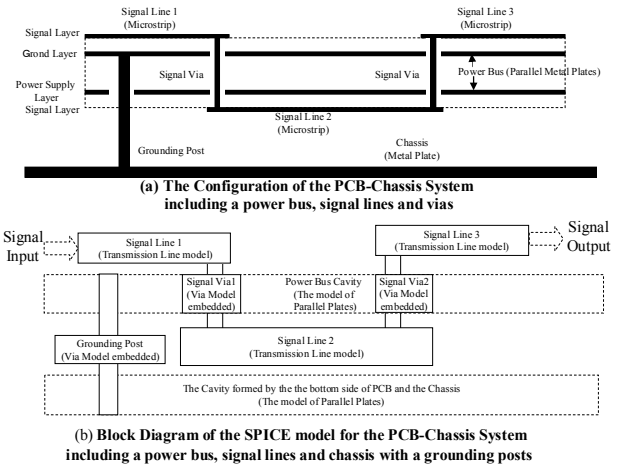
Figure 3. Configuration of the PCB-chassis system and its Block Diagram for the SPICE model.

III. COMPARISON WITH MEASUREMENTS

The SPICE model for the coupling between the signal lines and power bus was validated by comparing calculated results to experimental data. A four-layer test board (Test Board 1) consisting of copper planes and FR-4 material was built and a 4-port network analyzer was used to obtain the S-parameters between the power bus port, the input and output of the signal lines.

Figure 4 shows the configuration of the test board. The test board has signal traces on the 1st and 4th layers, the ground plane is on the 2nd layer, and the power plane is on the 3rd layer. The signal lines on the 1st and 4th layers are electrically connected with signal via structures as in the configuration of Figure 1(a). The dimensions of the test board are 20.0 cm x 10.0 cm and the distance between the power and ground planes is 1.0 mm. The signal traces are 0.2 mm above their respective planes and have a characteristic impedance of 50 ohms.

S_{21} (the insertion loss from the signal input to output with the power bus port open) and S_{31} (the insertion loss from signal input to power bus port with the signal output matched) were measured. The SPICE model for the test board was obtained according to the procedure introduced in the previous section and the calculated results were compared with the experimental data in Figures 5 and 6. The calculated results are consistent with the experimental data for S_{21} as well as S_{31}. The values of S_{21} are attenuated and those of S_{31} are amplified at the resonant frequencies of the power bus cavity. The discrepancies between measured and calculated values of S_{21} in the upper frequency ranges are likely due to the frequency dependence of the permittivity of the dielectric material, which is neglected in the SPICE model.
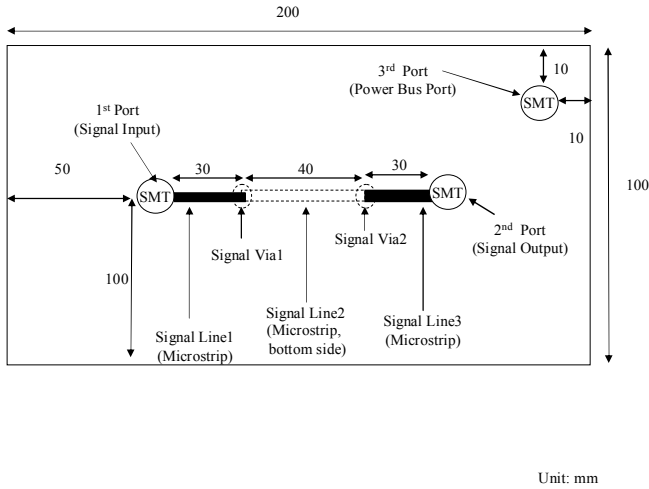
Figure 4. Test Board 1: for the measurement of the coupling between a signal line and a power bus due to via structures.
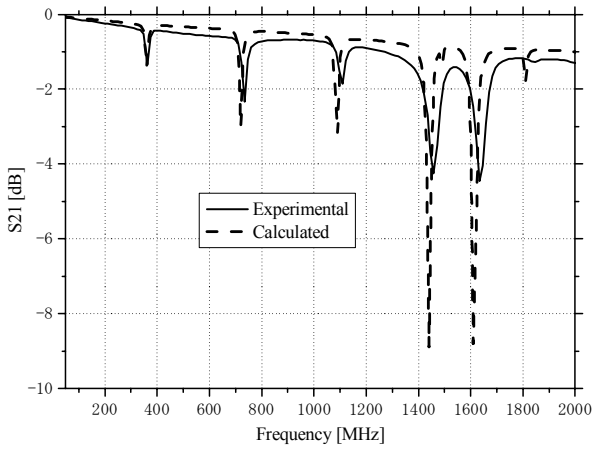
Figure 5. Comparison of the calculated results with corresponding experimental data from Test Board 1 (S21: signal input & output).

Next, the validity of the SPICE model for the PCB-chassis system was examined by comparing the calculated values for the radiated emissions with the corresponding experimental data. Another four-layer test board (Test Board 2) was built and the radiated emissions from the test board mounted on a chassis with different grounding post locations were measured in a 3-meter anechoic chamber.

Figure 7 shows the configuration of the test board. This test board also has signal traces on the 1st and 4th layers, a ground plane on the 2nd layer and a power plane on the 3rd layer. A 20-MHz clock oscillator and driver were mounted on the 1st layer and connected to one end of a 50-mm microstrip trace. The other

end was connected to a 50-mm segment of microstrip trace on layer 4 and the far end of this trace was connected to a third 50-mm microstrip trace back on layer 1. The dimensions of the test board were 21.0 cm x 14.0 cm and it was mounted on a 40.0-cm x 50.0-cm flat metal chassis using 1-cm grounding posts. A small battery box was attached to one edge of the PCB through a 4-cm cable with ferrite cores to suppress common-mode currents. The radiated emissions from the PCB without the chassis were measured from 30 MHz to 1 GHz. Then, these values were compared to the radiated emissions from the PCB mounted on the chassis with grounding posts. Notice that the PCB was mounted in a "return-on-top" configuration [3], which means that the power plane was sandwiched between the return plane and chassis, and that the grounding posts connected the return plane to the chassis through the power plane. Three grounding post configurations were evaluated: (a) 4 corner posts (4 grounding posts), (b) 4 corner posts and 2 more posts along the 2 longer edges (6 grounding posts), (c) 4 corner posts and 4 more posts along the 4 edges (8 grounding posts), (d) 4 corner posts and 16 more posts along the 4 edges. The grounding locations are shown in Figures 8(a), (b), (c) and (d). The vertical electric field was measured in the plane of the PCB and the maximum emissions at each frequency were reported. This orientation was selected because it is most likely to exhibit the effect of addition or cancellation of the fields along the edges of the PCB and the chassis cavity.
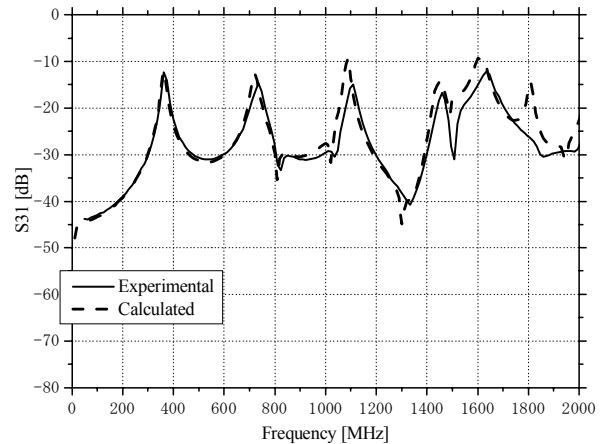
Figure 6. Comparison of the calculated results with corresponding experimental data from Test Board 1 (S31: signal input & power bus port).

As indicated by the plot in Figure 9, peaks in the radiated emissions from this test board with no chassis were observed every 20 MHz. The peak values with no chassis were used as a reference and the change in these peak values reflects the effect that the grounded chassis has on the radiated emissions at each frequency.
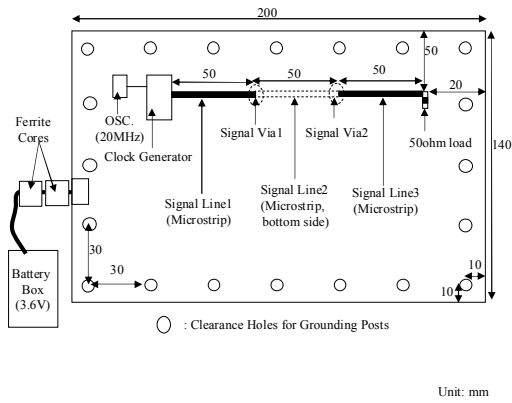
Figure 7. Test Board 2: for the measurement of the radiated EMI (a), and the grounding posts allocations investigated, (b), (c) and (d).

(a) **4 grounding posts**

(b) **6 grounding posts**

(c) **8 grounding posts**

(d) **20 grounding posts**

● : Positions of Grounding Posts
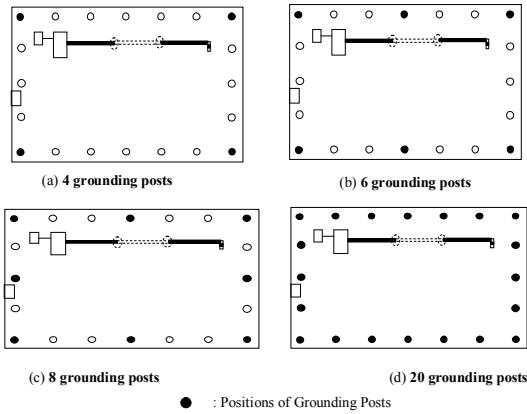
Figure 8. Grounding posts allocations investigated using the second test board , (a) 4 grounding posts, (b) 6 grounding posts, (c) 8 grounding posts, (d) 20 grounding posts.
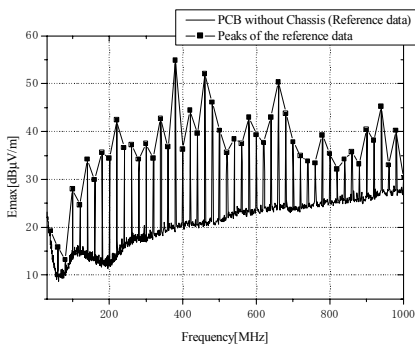
Figure 9. Radiated emissions from the second test board without chassis with the peak plot superimposed (Reference values).
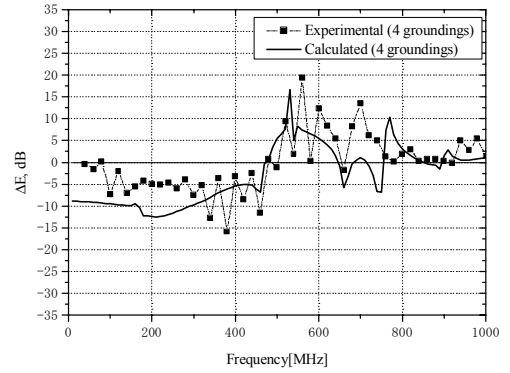
Figure 10. Differences of the radiated EMI from the reference values (Experimental and Calculated), 4 grounding posts.
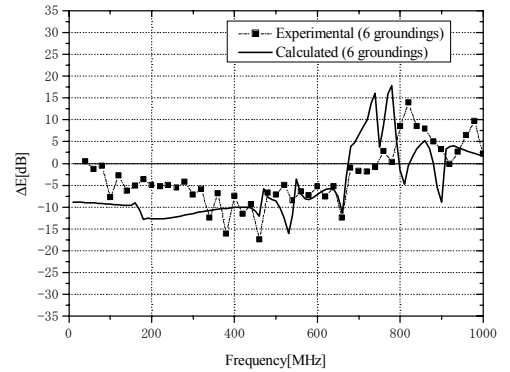
Figure 11. Differences of the radiated EMI from the reference values (Experimental and Calculated), 6 grounding posts.
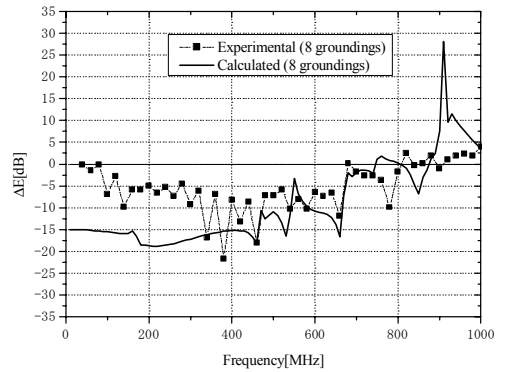
Figure 12. Differences of the radiated EMI from the reference values(Experimental and Calculated), 8 grounding posts.
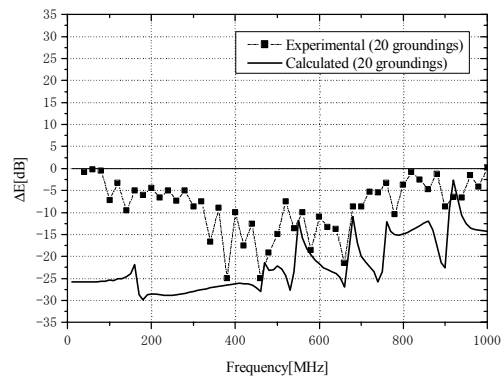
Figure 13. Differences of the radiated EMI from the reference values(Experimental and Calculated), 20 grounding posts.

Figures 10, 11, 12 and 13 show the comparisons of the calculated results with the corresponding experimental data for the 4, 6, 8 and 20 grounding posts, respectively. The results show the measured emissions tend to be attenuated by adding more grounding posts along the edges in addition to the posts at the 4 corners. The results also show that the calculated results are generally consistent with the measured data. Any discrepancies are likely due to the fact that the direct emission from the signal traces, the switching noise inside the power bus, the effects of the cable attached to the power bus, and the frequency dependence of the dielectric substrate were neglected in the SPICE model.

Notice that the radiated emissions corresponding to the 4 grounding post configuration are lower than the reference value at frequencies below 500 MHz (approximately the first resonant frequency of the cavity formed between the PCB and the chassis with grounding posts). The emissions tend to be higher than the reference in the upper frequency band. The radiated emissions corresponding to the 6 grounding post configuration are lower than the reference value at frequencies up to 700 MHz and the emissions corresponding to the 8 grounding post configuration are lower than the reference up to 900 MHz. The emissions corresponding to the 20 grounding post configuration are lower than the reference value at all measured frequencies.

The results suggest that it is a good idea to position grounding posts at the 4-corners and as many positions as possible to prevent resonances in the PCB-chassis cavity and reduce emissions over the widest possible frequency range. Ground post locations near the edge of the board are particularly effective because they help to ensure that the electric fields (and equivalent magnetic current sources) around the circumference of the power bus and cavity tend to cancel each other. The fields near the grounding posts in the chassis cavity have approximately the same amplitudes and opposite phases as the fields near the corresponding grounding points in the power bus.

When the PCB dimensions are small relative to the wavelength, the 4 corner grounding post locations are sufficient since the phase difference between the neighboring grounding posts is also small. When the length of the edges is comparable to a half-wavelength or longer, adding more grounding posts along the edges is recommended to reduce these phase differences and prevent resonances in the chassis cavity.

IV. CONCLUSIONS

SPICE modeling procedures for a PCB-chassis system with signal lines and via structures were proposed. First, the PCB consisting of the power bus, signal lines and via structures was modeled using an analytical model for the via structures. The calculated results for the coupling between a signal line and power bus were shown to be consistent with the experimental data obtained using a network analyzer. Next, the PCB-chassis system with grounding posts, signal lines and via structures was modeled. The grounding posts were modeled using the same technique used to model the via structures. The radiated emissions were then calculated using the SPICE model and equivalent magnetic current sources. The calculated results were again shown to be consistent with the corresponding experimental data. Both the calculated and experimental results show that the radiated emissions are reduced by employing a sufficient number of grounding posts along the edges of the PCB when the power plane is sandwiched between the return plane and the chassis.

REFERENCES

[1] G. Selli, C. Schuster and Y. Kwark, "Model-to-Hardware Correlation of Physics Based Via Models with the Parallel Plate Impedance Included," *Proc. of the 2006 IEEE International symposium on EMC*, Portland, OR, Aug. 2006, pp. 781-785.

[2] L. Tsang and Dennis Miller, "Coupling of Vias in Electronic Packaging and Printed Ciurcuit Board Structures With Fnite Ground Plae," *IEEE Trans. on Advanced Packaging*, vol. 26, no. 4, Nov. 2003, pp.375-384.

[3] N. Kobayashi, T. Harada, A.Shaik and T. Hubing, "An Investigation of the Effect of Chassis Connections on Radiated EMI from PCBs," *Proc. of the 2006 IEEE International Symposium on EMC*, Portland, OR, Aug. 2006, pp. 275-279.

[4] N. Kobayashi, T. Harada and T. Yaguchi, "Analysis of Multilayered Power-Distribution Planes with Via Structures using SPICE," *IEICE Technical Report, EMCJ2005-97*, pp.25-30.

[5] A. G. Williamson, "Radial/Coaxial-Line Junction: Analysis and Equivalent Circuits," *Int.. J. Electronics*, vol.58, no.1, 1985, pp.91-104.

[6] T. Harada et al, K. Asao, H. Sasaki and Y. Kami, "Power-Distribution-Plane Analysis for Multilayer Printed Circuit Boards with SPICE," *Proc.of 2000 IEMT/IMC Symposium*, pp.420-425, April, 2000.

[7] R. K. Hoffmann, "General Stripline Characteristics," *Handbook of Microwave Integrated Circuits*, Artech House, 1987, p.95-134.

[8] S. Ramo, J.R. Whinnery and T.Van Duzer, "Fields as Sources of Radiation," Fields and Waves in Communication Electronics, 3rd edition, John Wiley & Sons, 1994, p.614-617.